Spin Formability of High-Strength Aluminum Alloys for Aerospace Applications

Mary Cecilia Mulvaney, *PhD Candidate*, University of Virginia
NIA Graduate Research Assistant at NASA LaRC

Jim Fitz-Gerald, *Advisor*, University of Virginia
Karen Taminger, *Advisor*, NASA LaRC

VSGC Student Research Conference
April 13, 2023

Motivation

- Need for rapid manufacturing of stiffened cylindrical aerospace structures to meet demand
  - Launch vehicle cryogenic tank manufacturing relies on multipiece machined and welded construction, resulting in a 90% scrap rate and hundreds of meters of welds that add weight and inspection time[1]
  - Aircraft fuselage assembly requires tens of thousands of rivets to assemble skins, stiffeners, and ring frames[2]
- The integrally stiffened cylinder (ISC) process developed by NASA and MT Aerospace (Germany) unitizes the outer skin and longitudinal stiffeners of cylindrical structures[1]
  - Would reduce the manufacturing time, cost, weight, and part count of multiple aerospace structures[1]
- Critical need for Al alloys with sufficient formability to sustain ISC deformation and yield service properties that include high strength and damage tolerance

Al 6061 3-m diameter ISC formed in 1.5 hours at MT Aerospace (Germany) in 2019

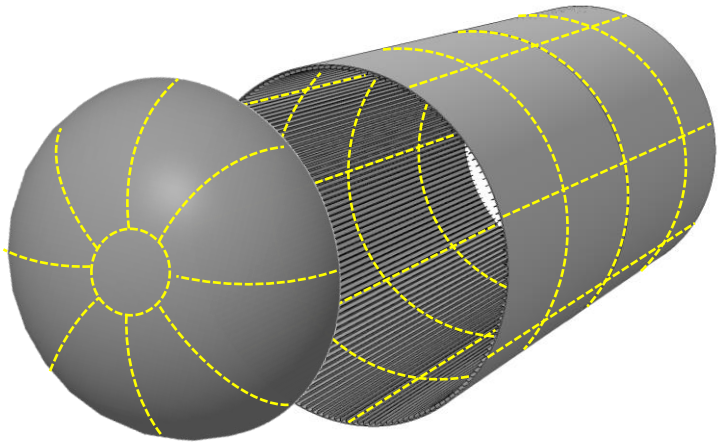

Notional cryogenic tank barrel from ISCs and spun dome: eliminates most welds (dotted yellow)

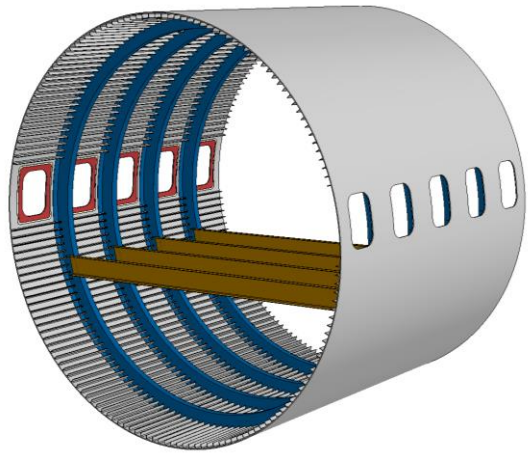

Notional aircraft fuselage section assembled from ISCs: eliminates tens of thousands of rivets

[1] Stoner, et al. "Cost-Benefit Analysis for the Advanced Near Net Shape Technology (ANNST) Method for Fabricating Stiffened Cylinders." NASA/TM-2016-219192.
[2] Hoffman et al. "Advanced Lightweight Metallic Fuselage Project Manufacturing Trade Study." NASA/TM-20210026758.

Materials and Methods

- Four Al alloys selected from different alloy families to establish the influence of strength, ductility, and hardening mechanisms on formability
- Conducted tensile tests to evaluate mechanical properties for correlation with forming trial results
- Utilized WF VUD-600 vertical forming machine recently installed at NASA LaRC for forming trials
  - Spin forming trials to convert 220-mm flat disks to 120-mm diameter cups in preparation for flow forming studies

Material	Al 6061[3]	Al 5083[4]	Al 2139[5]	Al 2050[6]
Nominal Composition (wt. %)	Al-1.0Mg-0.6Si-0.28Cu-0.2Cr	Al-4.4Mg-0.7Mn-0.15Cr	Al-5Cu-0.4Mn-0.5Mg-0.4Ag	Al-3.5Cu-1.0Li-0.4Mg-0.35Mn-0.45Ag-0.12Zr
RT Formability	High	Moderate	Unknown	Low
Strength / Heat Treat (HT)	Medium T6 strength with HT	Medium H32 strength with **no** HT	High T8 strength with HT	High T8 strength with HT
Hardening Mechanism	Precipitation hardened	Solid solution / work hardened	Precipitation hardened	Precipitation hardened

Al alloys evaluated by spin forming trials and tensile testing in the annealed, fully soft state (O-temper)

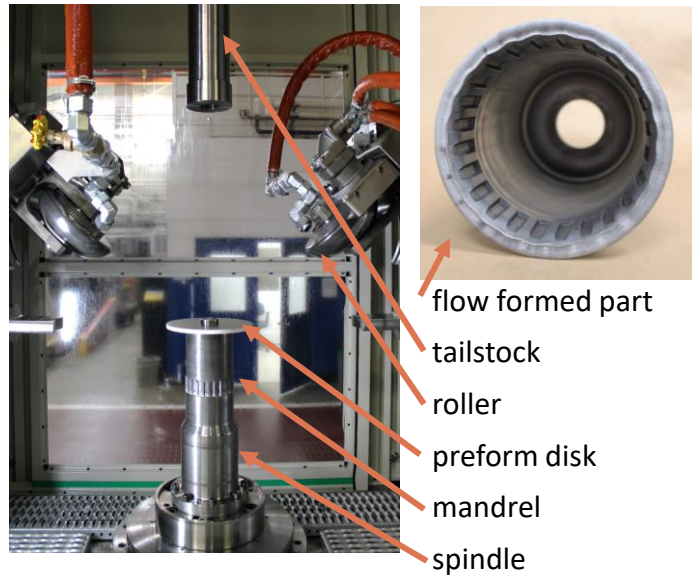

Interior of the WF VUD-600 vertical forming machine at NASA LaRC, with a flow formed demo part

[3] *AMS 4025N, SAE International, 2020.* [4] *AMS 4056H, SAE International, 2016.* [5] *AMS 4468, SAE International, 2017.* [6] *AMS 4413B, SAE International, 2019.*

Preform Disk Microstructures

- Initial preform microstructures were characterized with electron backscatter diffraction (EBSD)
- Al alloys 6061, 2139, and 5083 were recrystallized, while Al 2050 was unrecrystallized
- Al 5083 exhibited the smallest grain area and largest high angle grain boundary (HAGB) length
- Al 2050 exhibited the largest fraction of low angle grain boundaries (LAGB)

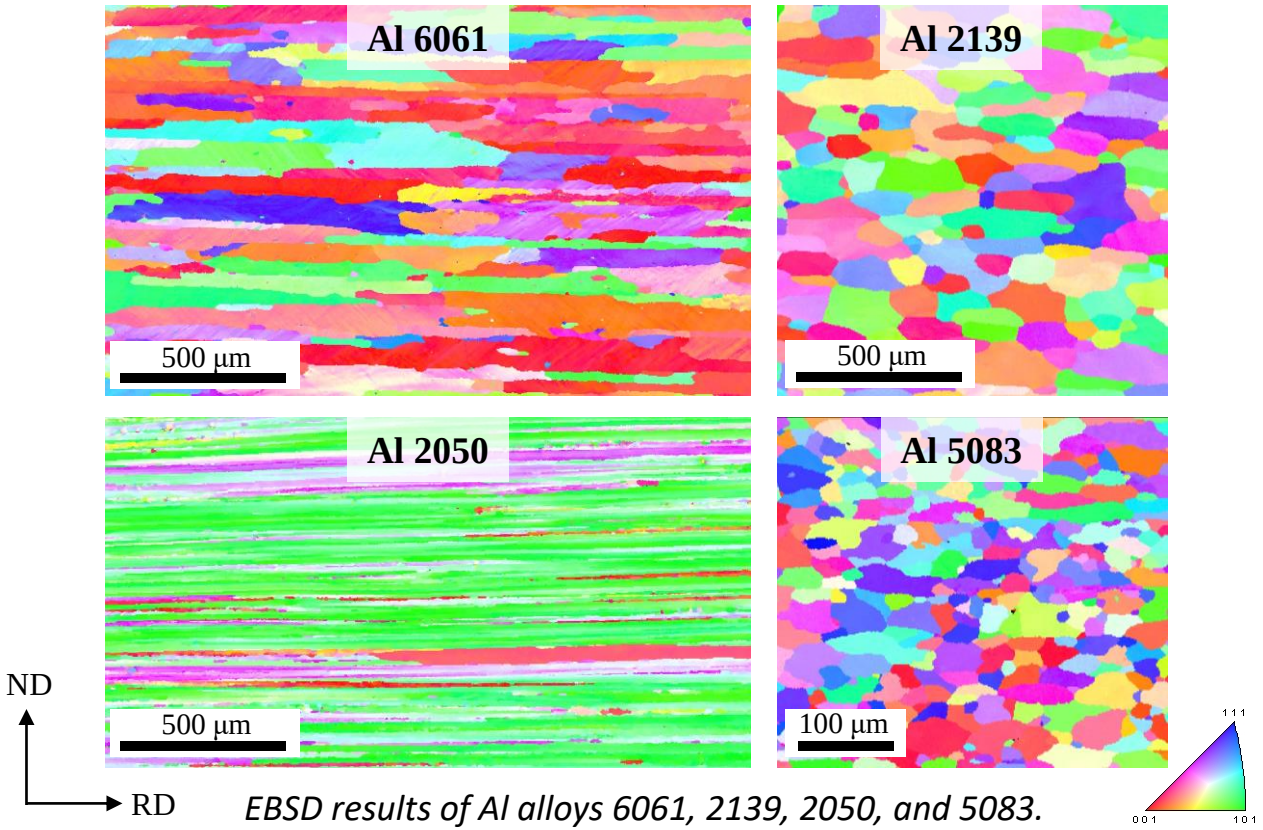

EBSD results of Al alloys 6061, 2139, 2050, and 5083. Note the smaller scale bar for Al 5083

Average:	**6061**	**5083**	**2139**	**2050**
Grain area (μm^2)	10400	370	7600	9100
HAGB length/image area (mm^{-1})	37	120	28	69
LAGB length/image area (mm^{-1})	9.9	11	4.1	19

EBSD grain size statistics from the microstructures of the alloy preforms

Preform Material Tensile Testing

- Tensile testing performed on annealed (fully soft) samples of Al alloys 6061, 5083, 2139, and 2050 with digital image correlation (DIC) strain mapping
- Area reduction (AR) calculated from necked region of fractured samples. All other tensile properties were calculated from the stress-strain curves

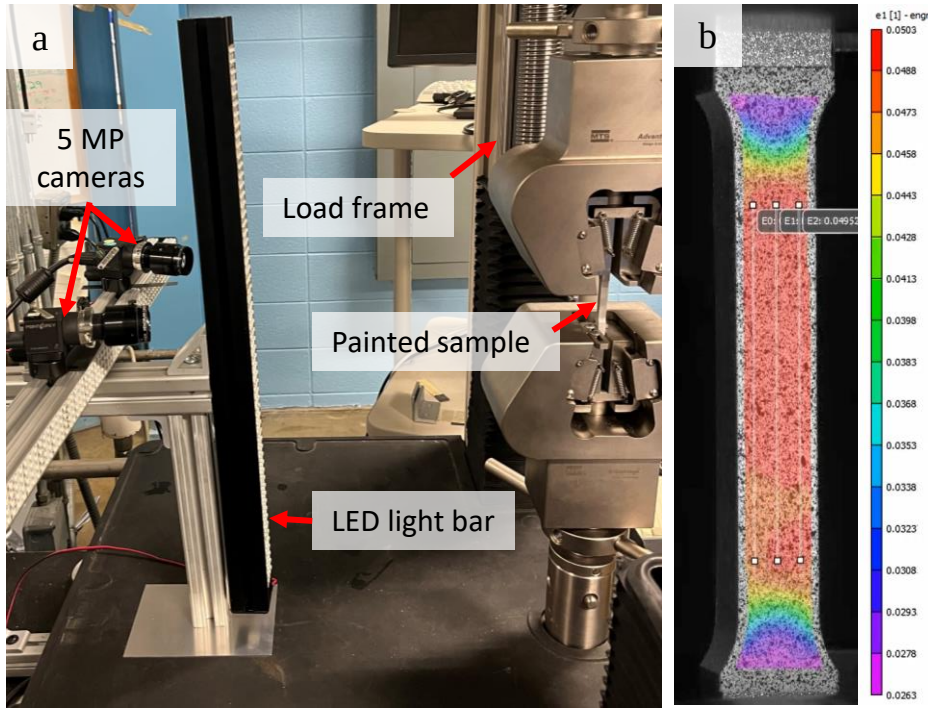

(a) Tensile testing setup with DIC strain mapping, (b) results from a sample at 5% strain

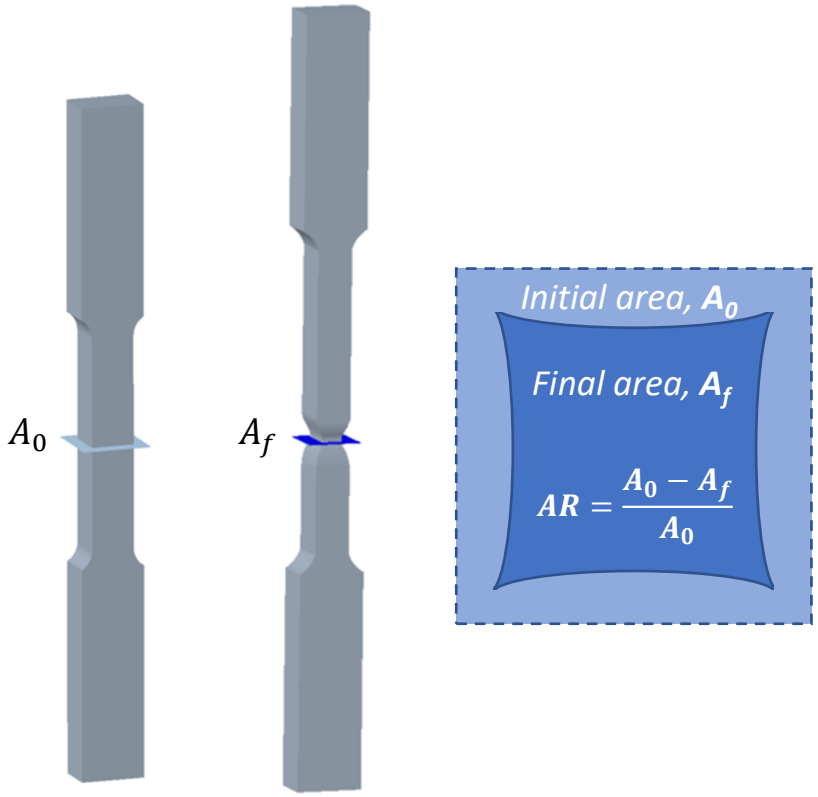

Schematic showing the initial (A_0) and final (A_f) cross sectional areas of a notional tensile sample and the equation for calculating AR

Preform Material Tensile Properties

- Al 6061 exhibited the highest ductility but lowest strength and work hardening
- Al alloys 2139, 2050, and 5083 exhibited roughly 2x the strength of Al 6061
- Al 2139 and Al 5083 showed 15% lower total elongation (e_{tot}) and 40% lower AR than Al 6061
- Al 2050 showed 40% lower e_{tot} and 50% lower AR than Al 6061

	Al 6061	Al 5083	Al 2139	Al 2050
Yield strength (MPa)	62	133	99	97
Ultimate tensile strength (MPa)	136	298	260	250
Work hardening coefficient, n	0.24	0.29	0.31	0.31
Total elongation, e_{tot} (%)	33.8	28.7	27.9	20.0
Area reduction, AR (%)	59	36	38	27

Mechanical properties measured from tensile testing

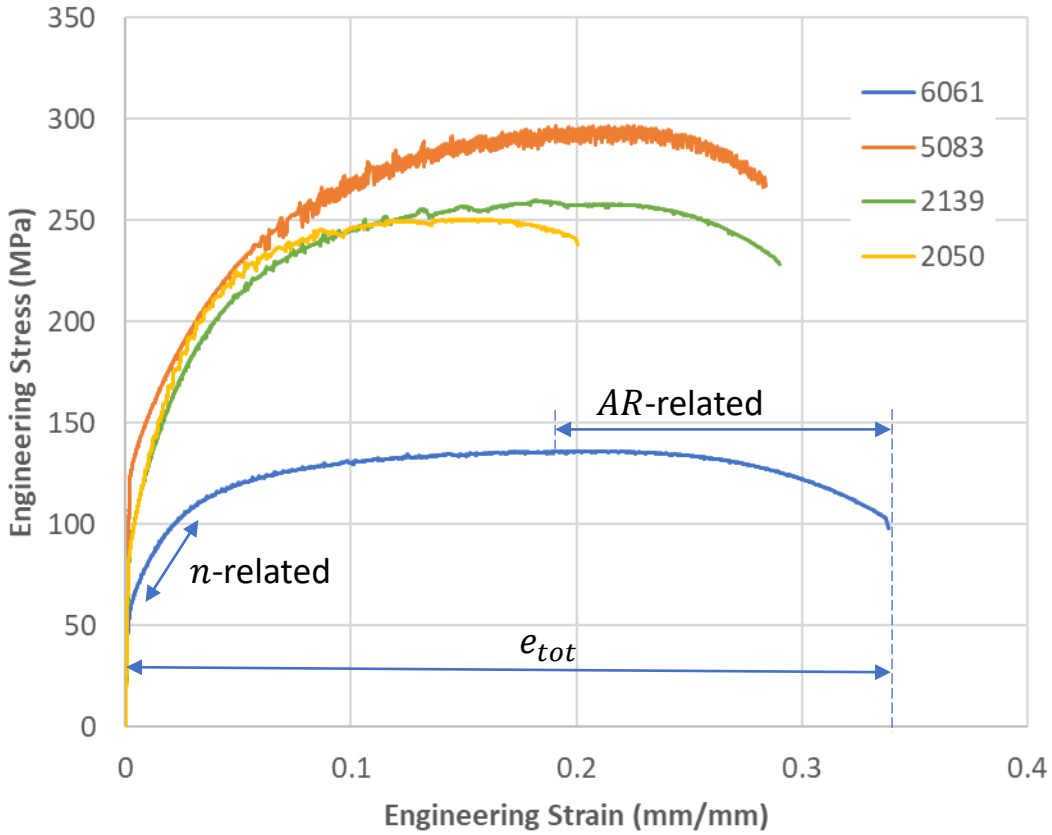

Engineering stress-strain curves for Al alloys 6061, 5083, 2139, and 2050

Spin Forming Trial Results – Al 6061

- Conducted spin forming trials using the VUD-600 to gain understanding of ambient temperature formability of Al alloys 6061, 5083, 2139, and 2050 in the annealed (fully soft) condition
  - Flood coolant/lubricant used to offset adiabatic heating
- Al 6061 formed successfully, conforming with target cup geometry without macroscale defects
  - Baseline program for Al 6061 used 5 downward + upward passes to form the cup
  - Inner mold line (IML) showed some orange peel but no microcracks

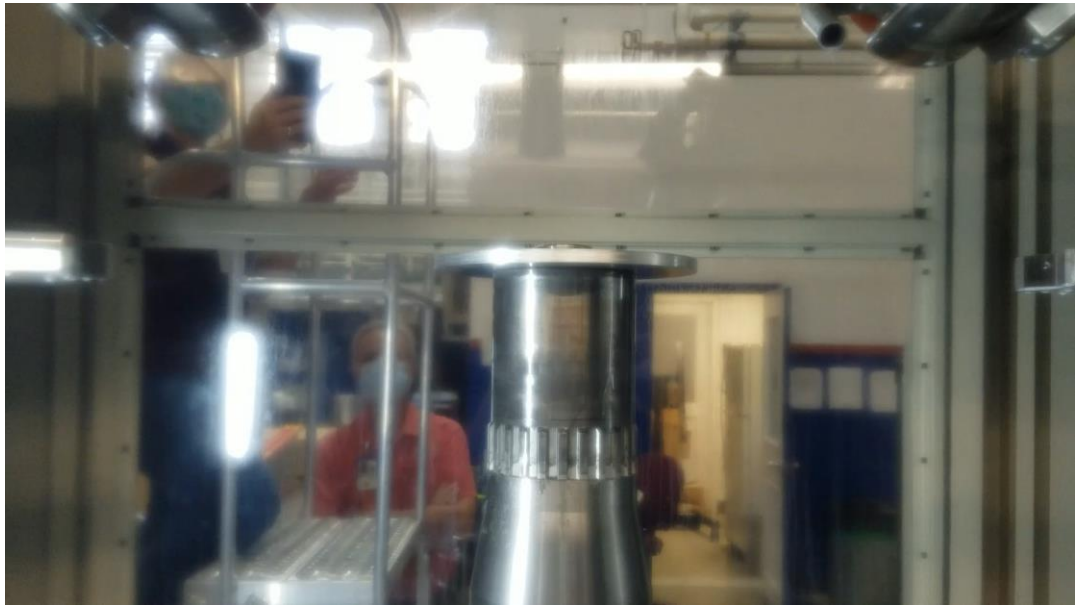

Video highlighting the five-step spin forming process with Al 6061. Coolant not used in the video for visual clarity

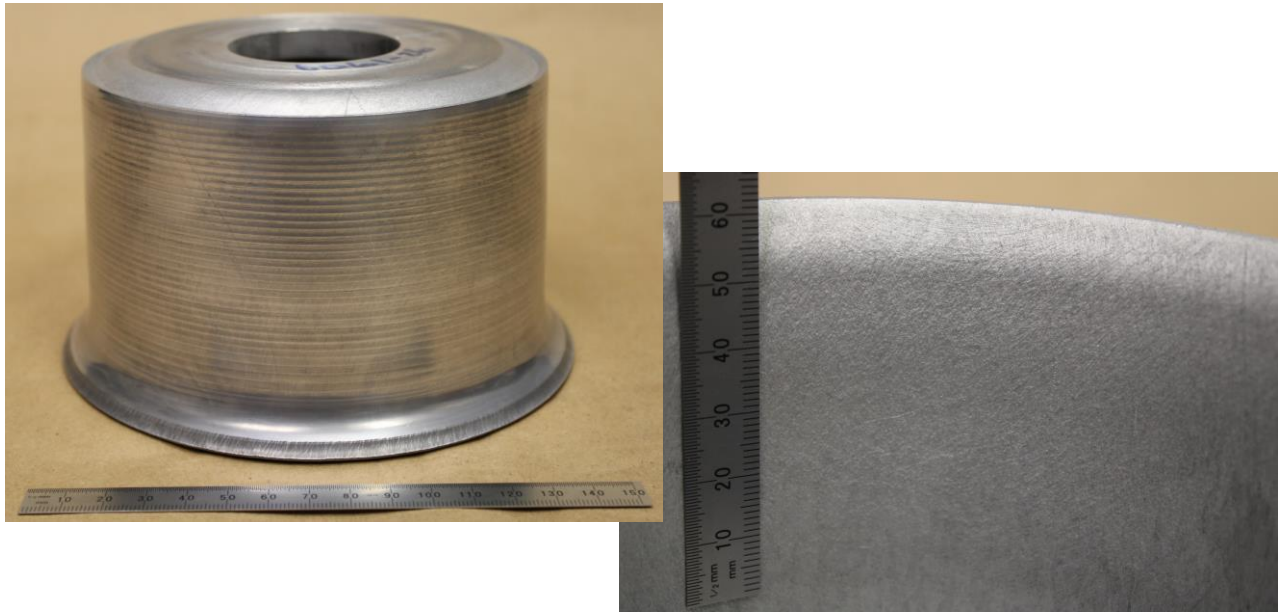

Successful Al 6061 spin formed part, with minor orange peel on the IML

Spin Forming Trial Results – Al 5083

- Tested various 5-pass and 6-pass spin forming paths to enable cup formation of Al 5083
- Severe defects emerged during Al 5083 forming trials, which included axial cracking, orange peel and microcracks on the IML, circumferential cracking, and lapping/flaking on the outer mold line (OML)

Axial cracking due to notch sensitivity of waterjet-cut edge

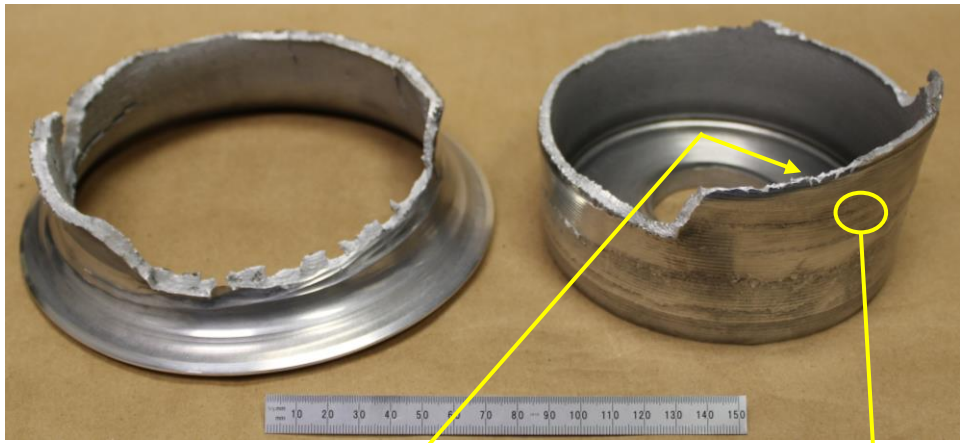

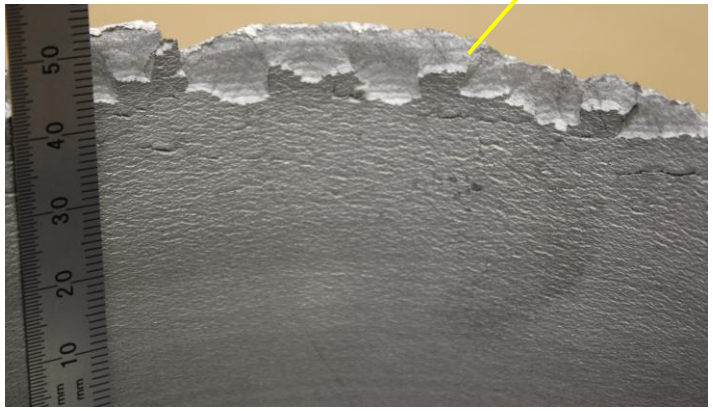

Orange peel; microcracks linked up to cause part failure; "beachmarks" on fracture surface; circumferential cracking; OML lapping

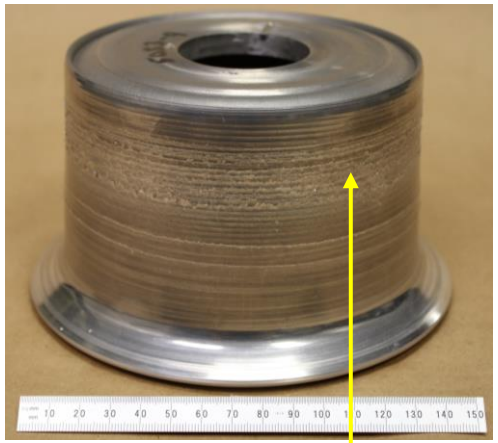

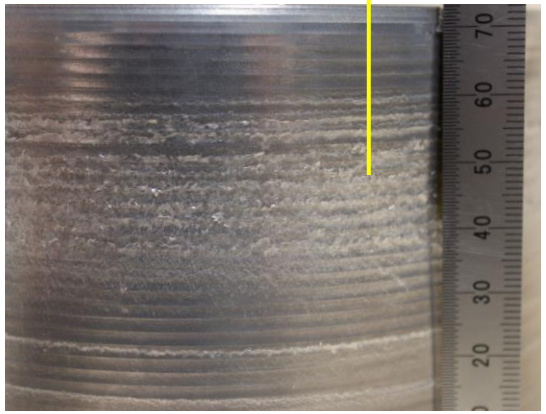

Intermediate annealing enabled cup formation; significant lapping on OML

Spin Forming Trial Results – Al 2139

- Al 2139 exhibited similar defects to Al 5083, most notably severe orange peel and microcracks on the IML and flange failure with “beachmarks” on the fracture surface

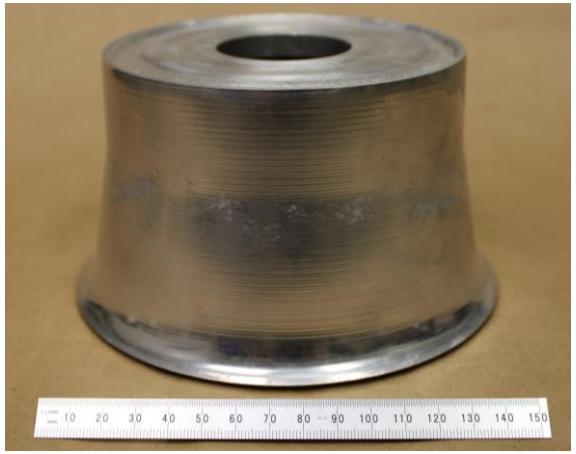

Part stopped prior to failure after 5 of 6 passes, showing orange peel and microcracks on IML

Part after the 6th forming pass showing flange separation and beachmarks on the fracture surface

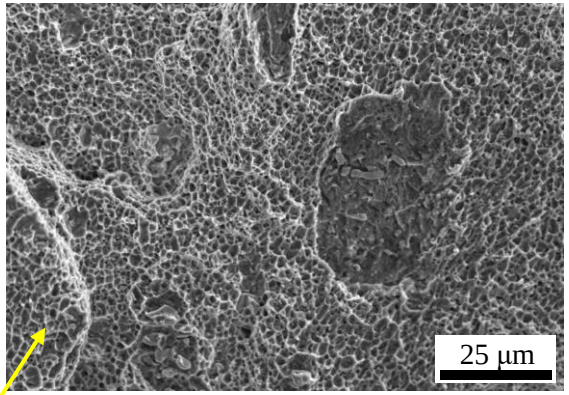

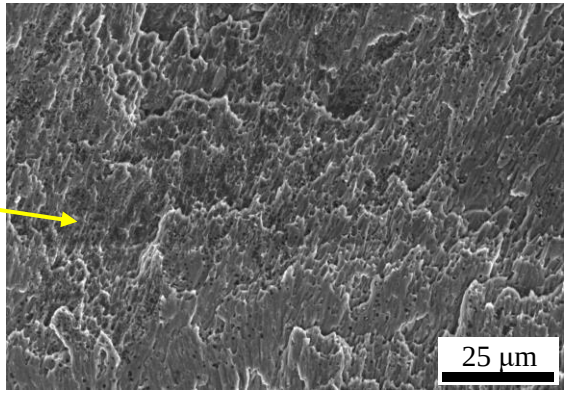

Beachmarks were comprised of alternating dimpled and shear regions

Spin Forming Trial Results – Al 2050

- Al 2050 failed during the 4th downward pass of 5 passes with flange cracking, orange peel and microcracking on the IML, and lapping and circumferential cracking on the OML
  - In contrast with Al 5083 and 2139, the fracture surface contained no beachmarks
- Microcracking on the IML differed between the rolling (RD) and transverse (TD) directions of the original plate
  - Larger cracks apparent on the TD walls of the cup

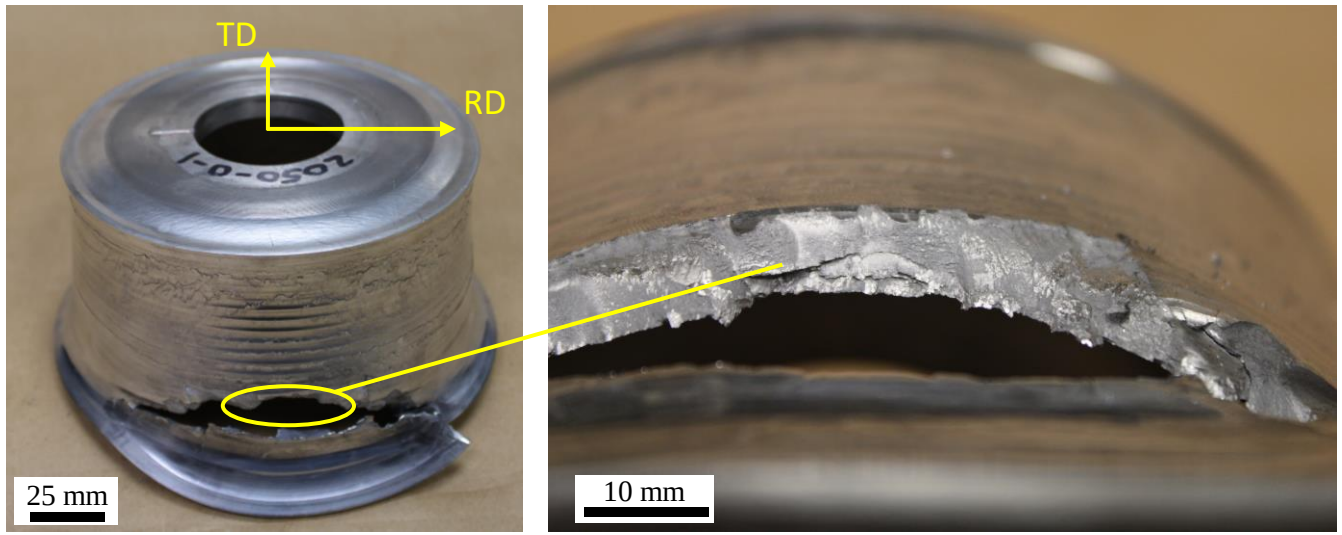

Al 2050 part that failed prematurely due to flange cracking, orange peel, and microcracks. The fracture surface does not show the more-ductile beachmark morphology as in Al alloys 2139 and 5083

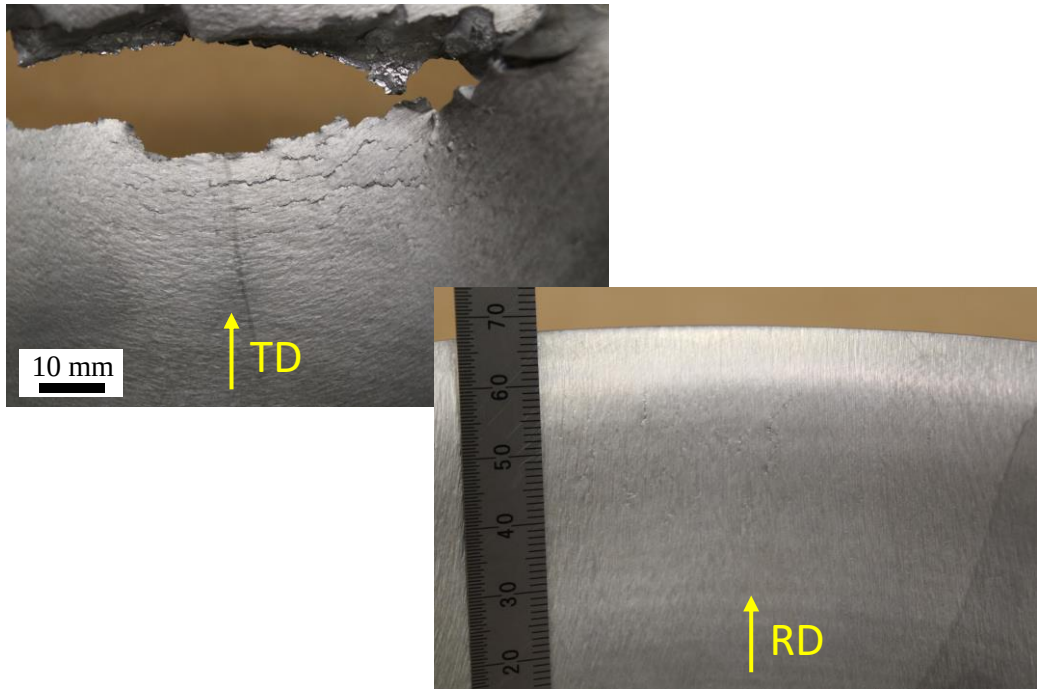

Microcracking differences between the RD and TD. Larger microcracks and the flange cracking appear in the TD

Discussion – Microstructure, Orange Peel, and Ductility

- Alloys with higher work hardening (n) values from tensile testing tended to show greater orange peel severity on the IML and also microcracking amidst the orange peel.

- Appearance of orange peel and microcracking was different for Al 2050 compared to the other alloys.
  - Attributed to the unrecrystallized microstructure, with grains elongated along the RD

- Beachmarks on fracture surfaces suggests low cycle fatigue failure as microcracks link up over multiple rotations. The beachmarks indicates more ductile failure compared to the flatter fracture of Al 2050 and correlates well with the e_{tot} values from tensile testing.

- Intermediate annealing of Al 5083 between after every two passes restored ductility, enabling cup formation. However, the most severe lapping on the OML was observed for this part.
  - Orange peel still appeared on the IML, but no microcracks

Conclusions

- Al 6061 exhibited excellent spin formability due to higher starting ductility and lower working hardening, which reduced orange peel and prevented microcracking.

- Al 2139 and Al 5083 exhibited very similar failures during spin forming, including orange peel and microcracks on the IML, as well as “beachmarks” on the fracture surface. These stem from higher work hardening coefficients than the other alloys, and higher e_{tot} than Al 2050.
  - Additional axial cracking, circumferential cracking, and lapping defects in Al 5083 parts

- Al 2050 showed preferential orange peel and microcracking in the TD due to strong preform texture and elongated grains. The fracture surface showed fewer ductile features than those of Al alloys 2139 and 5083, pointing towards its lower e_{tot} and AR tensile properties.

- Orange peel is a major impediment to ambient temperature forming of the high-strength alloys. Elevated temperature forming would lower work hardening, and downward-pass-only forming strategies would limit achievable strain.

Future Work

- Develop new spin forming schedule without upward passes to reduce tensile stresses on the IML (in progress). Eliminating upward passes should also reduce or eliminate lapping defects on the OML.

- Explore preheating of the Al alloy disks and forming without coolant to lower the flow stresses in the material. Elevated temperatures will lessen the tendency for orange peel and increase ductility.

- Compare forming experiments with simulations to understand strain evolution during forming and the relationship with orange peel, microcracking, and part failure.

- Expand mechanical testing to include compression and notched tensile testing to probe how other mechanical properties correlate with spin and flow formability.

- Conduct flow forming trials on spin formed cups to understand mechanical property correlations with flow formability. Determine maximum thickness reduction in a single pass for each alloy as a first step towards quantifying formability.

Acknowledgements

Special thanks to the NASA Advanced Air Transport Technology (AATT) project and the Virginia Space Grant Consortium (VSGC) for funding this work.

Thanks also to NASA LaRC's Advanced Materials and Processing Branch members for their support and collaboration in this research, especially:

Harold Claytor, Joel Alexa, and Teresa Oneil (VUD-600 operation); Wes Tayon and Dave Stegall (tensile testing and DIC setup); and Libby Urig (spin and flow forming discussions).

Thanks also to the Fitz-Gerald and Agnew lab groups at UVA for their support and feedback.

Special thanks to Jim Fitz-Gerald (UVA) and Karen Taminger (NASA LaRC) for their mentorship of this work!

Questions?